Electronic and magnetic properties of the Ag-doped Fe_3O_4 films studied by x-ray absorption spectroscopy

S. H. Liu, H. M. Tsai, C. W. Pao, J. W. Chiou, D. C. Ling, and W. F. Pong[a)]
Department of Physics, Tamkang University, Tamsui, Taiwan 251, Republic of China

M.-H. Tsai
Department of Physics, National Sun Yat-Sen University, Kaohsiung, Taiwan 804, Republic of China

H. J. Lin, L. Y. Jang, and J. F. Lee
National Synchrotron Radiation Research Center, Hsinchu, Taiwan 300, Republic of China

J. H. Hsu
Department of Physics, National Taiwan University, Taipei, Taiwan 106, Republic of China

W. J. Wang and C. J. Hsu
Department of Chemistry, Tamkang University, Tamsui, Taiwan 251, Republic of China

(Received 16 May 2006; accepted 4 July 2006; published online 30 August 2006)

The electronic and magnetic properties of Ag-doped Fe_3O_4 films were studied by x-ray absorption near-edge structure (XANES), extended x-ray absorption fine structure (EXAFS), and x-ray magnetic circular dichroism (XMCD) measurements. A comparison between the Ag *K*-edge EXAFS Fourier transform spectra of Ag-doped Fe_3O_4 and the Ag metal shows that Ag atoms aggregate into Ag granules. The O *K*-edge and Ag L_3-edge XANES spectra consistently indicate an electron transfer from the Fe_3O_4 host into Ag granules. The Fe $L_{3,2}$-edge XMCD spectra and hysteresis measurements reveal that Ag granules reduce the average magnetic moment of Fe ions and the saturation magnetization of Fe_3O_4. © *2006 American Institute of Physics*.
[DOI: 10.1063/1.2338889]

Magnetite (Fe_3O_4) is a well-known compound, which exhibits a first-order metal-insulator phase transition called the Verwey transition.[1] The valence states of Fe ions in the inverse-spinel-structured Fe_3O_4 have typically been assigned according to the chemical formula, $(Fe^{3+})_A[Fe^{2+}Fe^{3+}]_BO_4$, where the parentheses and square brackets refer to tetrahedral *A* and octahedral *B* sites,[2] respectively. Recently Versluijs *et al.*[3] and Chung *et al.*[4] explained the magnetoresistive effect of Fe_3O_4 by the hopping transport of spin-polarized electrons through a narrow domain wall pinned at the nanocontacts. Magnetite is a potential candidate for spintronics materials.[5] Hsu *et al.*[6] observed an anomalous magnetoresistance in Ag-doped Fe_3O_4 composite films and interpreted this finding as being caused by magnetic-field induced spin injection from Fe_3O_4 into Ag granules, which impedes the current. Partial substitution of Fe ions with magnetic[7] and nonmagnetic[8,9] metallic ions was also found to change the electronic and magnetic properties of Fe_3O_4. Al-doped Fe_3O_4 composite films have been investigated by Yang *et al.* using x-ray absorption near-edge structure (XANES) and x-ray magnetic circular dichroism (XMCD) measurements.[10] Since Ag differs from Al by having shallow 4*d* states, which may affect the magnetic properties of Fe_3O_4 and Ag was argued to form granules in Fe_3O_4, it is interesting to use x-ray spectroscopy to understand the electronic and magnetic properties of Ag-doped Fe_3O_4 composite films.

The O *K*- and Ag L_3-edge XANES, Ag *K*-edge extended x-ray absorption fine structure (EXAFS), and Fe $L_{3,2}$-edge XMCD were obtained using a high-energy spherical grating monochromator-20A, BL-15B, superconducting wavelength shifter-01C and Dragon-11A beamlines, respectively, at the National Synchrotron Radiation Research Center in Hsinchu, Taiwan. $Ag_x-(Fe_3O_4)_{1-x}$ ($x=0$, 0.05, and 0.1) composite films, denoted by $Ag(x)-Fe_3O_4$, were prepared by dc magnetron sputtering on thermally oxidized silicon (100) wafers with the composite targets made from Fe_3O_4 and Ag powder at a temperature of 350 °C. The preparation and characterization of the samples have been described elsewhere.[6]

Figure 1 presents the Fourier transform (FT) amplitudes of the EXAFS $k^3\chi$ data at the Ag *K*-edge for the $Ag(x)-Fe_3O_4$ films, the reference Ag metal, and AgO powder. The inset displays Ag *K*-edge EXAFS oscillations $k^3\chi$ data. The similarity between the FT spectra of the $Ag(x)-Fe_3O_4$ films and the Ag metal indicates that the local atomic environment of Ag atoms in $Ag(x)-Fe_3O_4$ films is similar to that in the Ag metal, but differ drastically from that in AgO. The first dominant peak in the FT spectra of the

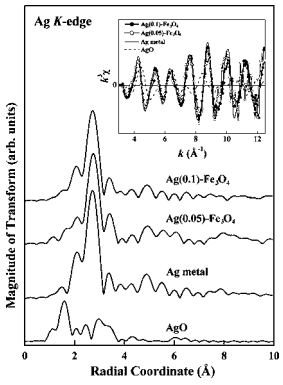

FIG. 1. Fourier transform amplitudes of the Ag *K*-edge EXAFS $k^3\chi$ data from $k=3.3$ to 12.5 $Å^{-1}$ for the $Ag(x)-Fe_3O_4$ films and the reference Ag metal and AgO powder. The inset plots the corresponding Ag *K*-edge EXAFS oscillations $k^3\chi$ data.

a)Author to whom all correspondence should be addressed; electronic mail: wfpong@mail.tku.edu.tw

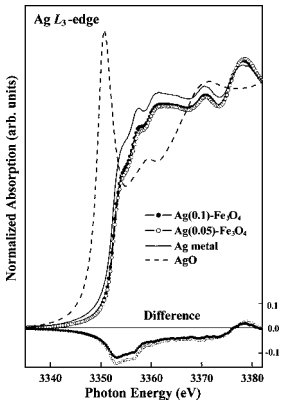

FIG. 2. Normalized Ag L_3-edge x-ray absorption spectra of the Ag(x)–Fe_3O_4 films and the reference Ag metal and AgO powder. The lower inset shows the difference near-edge spectrum between Ag(x)–Fe_3O_4 and the Ag metal.

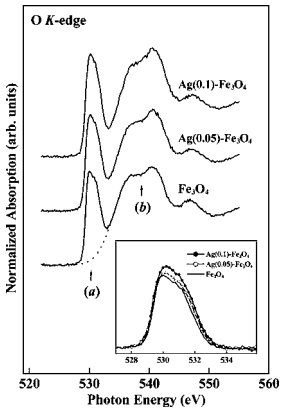

FIG. 3. Normalized O K-edge XANES spectra of the Ag(x)–Fe_3O_4 films. The inset displays the magnified near-edge features after background subtraction.

Ag(x)–Fe_3O_4 and the Ag metal is attributed to the nearest-neighbor Ag–Ag bond length (i.e., radial distance) of ~2.89 Å.[11] The same Ag–Ag bond lengths in the spectra of Ag(x)–Fe_3O_4 and the Ag metal strongly suggests that Ag atoms aggregate into Ag granules in the Ag(x)–Fe_3O_4 films. The distinctly different Ag–Ag bond lengths in Ag(x)–Fe_3O_4 and AgO show no evidence of Fe ions partially substituting by Ag ions and in fact that Ag granules are dominantly in contact with Fe ions instead of O ions. Additional Fe K-edge EXAFS measurements for Ag(x)–Fe_3O_4 (not shown) show that the local atomic environment of the Fe atoms in the Ag(x)–Fe_3O_4 (x=0.05 and 0.1) films closely resembles that of the Fe_3O_4 (x=0) sample, which indicates that addition of Ag does not change the inverse spinel structure of the Fe_3O_4 composite films.

Figure 2 shows the normalized Ag L_3-edge XANES spectra of the Ag(x)–Fe_3O_4 films, Ag metal, and AgO powder. According to the dipole-transition selection rule, the Ag L_3-edge XANES spectra predominantly reflect transitions from the Ag $2p$ core level to unoccupied Ag $4d/5s$-derived states.[12] As shown in Fig. 2, the spectral features of the Ag(x)–Fe_3O_4 films closely resemble those of the Ag metal but differ clearly from those of AgO; in particular, the near-edge features of the Ag(x)–Fe_3O_4 films and the Ag metal (Ag^{0+}) lie much higher energy than that of AgO (Ag^{2+}), which agrees with earlier observation by Kolobov *et al.*[13] The result of the formation of metallic Ag granules and the absence of the Ag–O bonding in the Ag(x)–Fe_3O_4 films is consistent with the Ag K-edge EXAFS observation. The bottom of Fig. 2 displays the difference Ag L_3-edge near-edge spectrum between the Ag(x)–Fe_3O_4 and the Ag metal, which shows reduction of the density of unoccupied Ag $4d/5s$ states in Ag(x)–Fe_3O_4. This result suggests an electron transfer from the Fe_3O_4 host into the Ag granules. The direction of charge transfer suggests that at the Fe_3O_4/Ag granule interfaces, the interface dipoles point towards the Ag granule, as a result that the electrostatic potential in the Ag granule is lowered relative to that in the Fe_3O_4 host. The direction of dipoles implies that Ag atoms at the interfaces are dominantly in contact with Fe ions, which have positive effective charges. This argument is consistent with the observation of the absence of AgO by EXAFS measurement.

Figure 3 displays the normalized O K-edge XANES spectra of the Ag(x)–Fe_3O_4 films. The O K-edge XANES spectra reflect transitions to unoccupied $2p$-derived states of oxygen and the states of neighboring ions, which have significant p-symmetry components projected onto the O sites and usually hybridize with O $2p$ states. Features ***a*** and ***b*** are mainly unoccupied hybridized states between O $2p$ and relatively narrow $3d$ and broader $4sp$ bands of Fe ions, respectively. The inset in Fig. 3 magnifies feature ***a*** for the Ag(x)–Fe_3O_4 films after the background represented by a best-fitted Gaussian curve (dashed line) has been subtracted. The intensity of feature ***a*** increases slightly with the Ag concentration x, which indicates that Ag increases slightly the unoccupied O $2p$-Fe $3d$ states in Ag(x)–Fe_3O_4. This trend is opposite to that of Al(x)–Fe_3O_4, for which the intensity of feature ***a*** decreases as the Al concentration x increases.[10]

Figure 4(a) presents the normalized Fe $L_{3,2}$-edge XANES and XMCD (i.e., I_+-I_-) spectra of the Ag(x)–Fe_3O_4 films. I_+ (I_-) refers to the absorption spectrum obtained by projecting the spin of the incident photons parallel (antiparallel) to the direction of the Fe $3d$ majority spin. The general line shapes of the Fe $L_{3,2}$-edge XANES and XMCD spectra of these Ag(x)–Fe_3O_4 films are similar to those of Fe_3O_4 reported elsewhere.[10,14–17] Figure 4(b) displays a magnified view of the XMCD features at the Fe L_3 edge, which shows two prominent negative and one positive XMCD features.

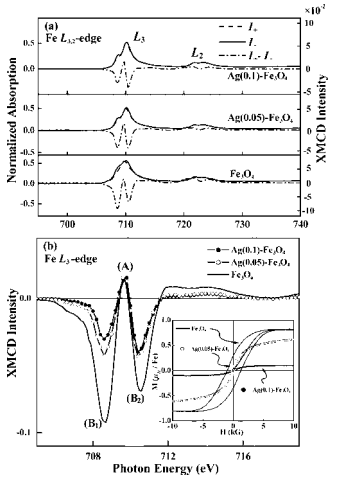

FIG. 4. (a) Normalized Fe $L_{3,2}$-edge XANES and XMCD spectra of the Ag(x)–Fe_3O_4 films. (b) is the magnified view of XMCD features of the Ag(x)–Fe_3O_4 films at the Fe L_3-edge. The inset plots hysteresis loops of the Ag(x)–Fe_3O_4 films at room temperature.

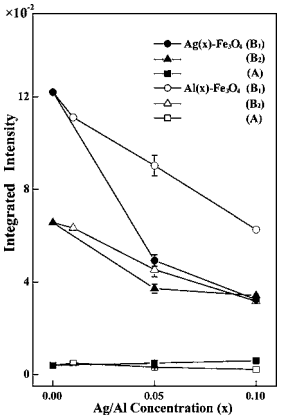

FIG. 5. Representative integrals of the two negative and one positive features in Fe L_3-edge XMCD spectra as functions of x for $Ag(x)-Fe_3O_4$ and $Al(x)-Fe_3O_4$ (Ref. 10), respectively.

Whether Fe ions have Fe^{2+} and Fe^{3+} charge orderings or a fluctuating mixed valence state in the inverse-spinel-structured Fe_3O_4 remains controversial.[18,19] Kuiper *et al.* based on the Fe^{2+} and Fe^{3+} charge orderings attributed the two negative features to the Fe ions at the octahedral B sites, namely, $Fe^{2+}(B)$ and $Fe^{3+}(B)$, and the positive feature to the Fe ions at the tetrahedral A sites, $Fe^{3+}(A)$.[14] On the other hand, Yang *et al.*[10] attributed the two negative XMCD features, which have a separation of approximately 2 eV in close agreement with that of the twin-peak feature a in the O K-edge XANES spectra, to the spin-polarized Fe $3d$ e_g and t_{2g} bands of B site Fe ions and the positive XMCD feature in between to the remnant intensity of the $3d$ states of the A-site Fe ions, which is not overshadowed by the two negative features. Figure 4(b) demonstrates that the intensities of the XMCD features decrease significantly as the Ag concentration increases, which indicates that the embedding of Ag granules in Fe_3O_4 reduces the overall magnetic moment of Fe ions. The interpretation of the decrease of the XMCD intensity as a reduction of the overall magnetic moment of the Fe ions is confirmed by the magnetic hysteresis measurements of $Ag(x)-Fe_3O_4$ shown in the inset of Fig. 4(b) and the magnetic force microscopic measurement (not shown). The hysteresis loops show that the saturation magnetic moment of the Fe ions in a field of 10 kG is reduced from $0.8\mu_B$ for undoped Fe_3O_4 down to about $0.6\mu_B$ and $0.1\mu_B$ for $Ag(x)-Fe_3O_4$ with $x=0.05$ and 0.1, respectively. It is also interesting to note that the saturation magnetic moment drops roughly as a quadratic function of x. In addition, the coercivity is decreased correspondingly from ~720 G for Fe_3O_4 to 260 and 85 G for $Ag(x)-Fe_3O_4$ with $x=0.05$ and 0.1, respectively. The average magnetic moment of the Fe ions in Fe_3O_4 is less than the atomic value of $2.0\mu_B$, which is due to the fact that Fe $3d$ orbitals hybridize with O $2p$ orbital and that Fe^{3+} ions align antiferromagnetically at the A and B sites.

Figure 5 plots the integrals of the two negative XMCD features from 703.3 to 709.4 eV (indicated as B_1) and from 709.8 to 711.6 eV (B_2) and the positive XMCD feature from 709.4 to 709.8 eV (A) in the Fe L_3-edge XMCD spectra as functions of the amount of Ag in $Ag(x)-Fe_3O_4$ and the amount of Al in the $Al(x)-Fe_3O_4$ (Ref. 10) to compare the effect of Ag and Al dopants on the magnetic properties of Fe_3O_4. It shows that the intensities of negative XMCD features decrease significantly and the intensity of the positive XMCD feature remains nearly constant (decreases slightly) as the Ag (Al) concentration increases, revealing that both Ag and Al dopings reduce the overall magnetic moment of Fe ions in the Fe_3O_4. The integrated intensity of feature B_1 at the Fe L_3-edge XMCD of $Ag(x)-Fe_3O_4$ decreases more rapidly than that of $Al(x)-Fe_3O_4$, which can be attributed to a different structural property of the Al dopants.

The ferromagnetic materials are composed of magnetic domains. The lining up of Fe spins within a given domain may be due to delocalized majority-spin (↑ spin) Fe $3d$ e_g states by analogy with doped manganites.[20] The embedded Ag granules have three plausible effects on the electronic and magnetic properties of Fe_3O_4. The first effect is that the conduction, i.e., itinerant, states of Ag granules can couple with delocalized ↑-spin Fe $3d$ e_g states, which reduces the spin polarization of these Fe $3d$ e_g states and consequently weaken the magnetic coupling of Fe spins. This coupling between Ag itinerant and delocalized Fe $3d$ ↑-spin e_g states also reduces greatly the resistivity of the films as observed by Hsu *et al.*[6] The second effect is that the interface-dipole induced electron transfer stated previously reduces the spin moment of Fe ions. The third effect is that the embedded Ag granules may hinder the lining up of the polarization of magnetic domains when a magnetic field is applied, because the lining up of magnetic domains concerns the movement of domain boundaries. These combined effects cause the saturation magnetic moment to drop so rapidly with x as shown in the magnetic hysteresis measurement.

This work was supported by the National Science Council of the Republic of China under Contract No. NSC 94-2112-M-032-013.

[1] E. J. Verwey and P. Haayman, Physica (Amsterdam) **8**, 979 (1941).
[2] See B. D. Cullity, *Introduction to Magnetic Materials* (Addison-Wesley, Menlo Park, CA, 1972).
[3] J. J. Versluijs, M. A. Bari, and J. M. D. Coey, Phys. Rev. Lett. **87**, 026601 (2001).
[4] S. H. Chung, M. Muñoz, N. García, W. F. Egelhoff, and R. D. Gomerz, Phys. Rev. Lett. **89**, 287203 (2002).
[5] G. A. Prinz, Science **282**, 1660 (1998).
[6] J.-H. Hsu, S.-Yi Chen, W. M. Chang, T. S. Jian, C. R. Chang, and S. F. Lee, J. Appl. Phys. **93**, 7702 (2003).
[7] V. N. Antonov and B. N. Harmon, Phys. Rev. B **67**, 024417 (2003).
[8] W. F. J. Fontijn, P. J. van der Zaag, M. A. C. Devillers, V. A. M. Brabers, and R. Metselaar, Phys. Rev. B **56**, 5432 (1997).
[9] V. N. Antonov, B. N. Harmon, and V. P. Antropov, Phys. Rev. B **64**, 134410 (2001).
[10] C. K. Yang, J. W. Chiou, H. M. Tsai, C. W. Pao, J. C. Jan, S. C. Ray, C. L. Yeh, K. C. Huang, H. C. Hsueh, W. F. Pong, M.-H. Tsai, H. H. Hsieh, H. J. Lin, T. Y. Hou, and J. H. Hsu, Appl. Phys. Lett. **86**, 062504 (2005).
[11] D. Lützenkirchen-Hecht and R. Frahm, Physica B **283**, 108 (2000).
[12] W. Drube, T. K. Sham, A. Kravtsova, and A. V. Soldatov, Phys. Rev. B **67**, 035122 (2003).
[13] A. V. Kolobov, A. Rogalev, F. Wilhelm, N. Jaouen, T. Shima, and J. Tominaga, Appl. Phys. Lett. **84**, 1641 (2004).
[14] P. Kuiper, B. G. Searle, L.-C. Duda, R. M. Wolf, and P. J. van der Zaag, J. Electron Spectrosc. Relat. Phenom. **86**, 107 (1997).
[15] H. J. Kim, J. H. Park, and E. Vescovo, Phys. Rev. B **61**, 15284 (2000).
[16] P. Morrall, F. Schedin, G. S. Case, M. F. Thomas, E. Dudzik, G. van der Laan, and G. Thornton, Phys. Rev. B **67**, 214408 (2003).
[17] J. Chen, D. J. Huang, A. Tanaka, C. F. Chang, S. C. Chung, W. B. Wu, and C. T. Chen, Phys. Rev. B **69**, 085107 (2004).
[18] F. Walz, J. Phys.: Condens. Matter **14**, R285 (2002).
[19] J. García and G. Subías, J. Phys.: Condens. Matter **16**, R145 (2004).
[20] M.-H. Tsai, Y.-H. Tang, H. Chou, and W. T. Wu (unpublished).